MAGNETIC RESONANCE

Deep gray matter changes in relapsing-remitting multiple sclerosis detected by multi-parametric, high-resolution magnetic resonance imaging (MRI)

Ali Al-Radaideh[1] · Imad Athamneh[2] · Hadeel Alabadi[2] · Majed Hbahbih[3]

Abstract

Objectives To investigate a variety of magnetic resonance imaging (MRI) quantitative metrics, which reflect different aspects of microstructural damage in deep gray matter (dGM) regions and white matter T2 lesions in patients with relapsing-remitting multiple sclerosis (RRMS), and to determine the level of pathological interconnection between these two entities as well as their association with clinical disability.

Methods We recruited thirty RRMS patients along with thirty age-matched healthy controls (HCs). Both groups were scanned at 3 T MRI using 3D high-resolution T1-, T2-, and T2*-weighted, magnetization transfer (MT)–prepared gradient echo for MT ratio (MTR) mapping, and eight repeats of T1-weighted images acquired at different inversion times to create T1 maps. dGM structures were segmented from T1-weighted images using FreeSurfer, WM-T2 lesions were extracted from T2-weighted images, and iron maps were calculated from the phase part of the T2*-weighted sequence. Extracted dGM MRI indices were compared between both groups. In the RRMS group, dGM MRI indices were correlated with those of WM-T2 lesions, expanded disability status scale, and disease duration.

Results dGM volumetric metrics of RRMS patients were significantly ($p < 0.01$) smaller than those of HCs and showed a significant moderate association with lesions' load ($p < 0.05$) and lesions' iron concentration ($p < 0.01$). dGM MTRs of RRMS patients were significantly ($p < 0.01$) smaller than those of HCs and showed a significant ($p < 0.01$) moderate correlation with lesion T1 times. While T1 changes in some dGM regions of RRMS patients associated weakly with those of T2 lesions, dGM iron concentration did not show any association with any of lesions' metrics. Furthermore, lesions' MTR changes did not show any association with any dGM metrics. Most dGM metrics did not show any correlation with disease severity. Contrarily, most lesions' metrics showed weak association with disease severity.

Conclusions dGM changes occur in a non-uniform pattern and, almost, do not link directly to MS disease severity. Contrarily, most WM-T2 lesions' metrics tend to correlate with MS disease severity better than those of dGM.

Key Points
• *Deep gray matter (dGM) structures are very much involved in the MS disease process and quite substantial neurodegeneration is undergone during the relapsing-remitting phase of the MS disease.*
• *Deep gray matter (dGM) quantitative changes occur in a non-uniform and non-linked pattern and, except for CN's iron deposition, do not directly associate with the MS disease severity.*
• *Most white matter T2 lesions' metrics tend to correlate with MS disease severity better than those of dGM structures.*

Keywords Magnetic resonance imaging · Relapsing-remitting multiple sclerosis · Metrics · Deep gray matter · Iron

✉ Ali Al-Radaideh
  Ali.Radaideh@hu.edu.jo

1   Department of Medical Imaging, Faculty of Applied Medical Sciences, The Hashemite University, Zarqa, Jordan

2   Department of Radiology, King Hussein Medical Center, Jordanian Royal Medical Services, Amman, Jordan

3   Department of Internal Medicine, Neurology, King Hussein Centre, Jordanian Royal Medical Services, Amman, Jordan

Abbreviations

3D	3 Dimensions
3T	3 Tesla
CN	Caudate nucleus
CSF	Cerebrospinal fluid
dGM	Deep gray matter
DTI	Diffusion tensor imaging
EDSS	Expanded disability status scale
eTICV	Estimated total intracranial volume
Fe	Iron
FLAIR	Fluid-attenuated inversion recovery
FLASH	Fast low-angle shot
FLIRT	Functional magnetic resonance imaging of the brain software library Linear Image Registration Tool
FS	Functional system
FSL	Functional magnetic resonance imaging of the brain Software Library
g	Gram
GM	Gray matter
GP	Globus pallidus
HCs	Healthy controls
LUT	Look-up-table
MPRAGE	Magnetization prepared–rapid acquisition gradient echo
MRI	Magnetic resonance imaging
MS	Multiple sclerosis
MT	Magnetization transfer
MTR	Magnetization transfer ratio
NAGM	Normal-appearing gray matter
PPMS	Primary progressive multiple sclerosis
PT	Putamen
RF	Radiofrequency
RMS	Royal Medical Services
RRMS	Relapsing-remitting multiple sclerosis
SPMS	Secondary progressive multiple sclerosis
SPSS	Statistical Package for Social Sciences
TE	Echo time
TH	Thalamus
TR	Repetition time
WM	White matter
WM-T2LL	White matter T2 lesion load
μg	Microgram

Introduction

The involvement of deep gray matter (dGM) structures in multiple sclerosis (MS) disease is of particular interest because they are involved in all major functional circuits in the brain [1]. dGM damage has been correlated with fatigue, higher expanded disability status scale (EDSS) scores, and cognitive impairment in MS patients [2, 3].

The extent of damage to the microstructure of brain tissues can also be expressed as a reduction in the efficiency of protons bound to macromolecules in brain parenchyma to exchange magnetization with free water [4]. The latter is measured using the magnetization transfer ratio (MTR) technique. Reduced MTR in normal-appearing gray matter (NAGM) is present in all MS clinical phenotypes [5–8] but is greatest in secondary progressive MS (SPMS) and primary progressive MS (PPMS) [9]. Demyelination, edema, gliosis, and axonal and neuronal loss can cause an abnormal shift in proton's relaxation times (T1, T2, T2*) even if the tissues appear normal on imaging. This may bear clinical significance in terms of predicting disease progression and long-term disability in MS. Gray matter (GM) atrophy, which contributes to the whole brain atrophy in patients suffering from MS, reflects a combination of demyelination, neurite transection [10], and reduced synapse or glial densities [11, 12]. Different MRI-based morphometric techniques (manual, semi-automated, and automatic) have been implemented to measure the regional and global brain atrophy. Furthermore, accumulation of brain iron in the dGM has been suggested as a biomarker of neurodegeneration and an inducer of oxidative stress in the brain, which reflects the extent of tissue damage. Iron accumulation in the dGM of MS patients was found to occur during the earliest stages of the MS disease [13]. MS lesions on T2-weighted brain images appear as bright areas and are often referred to as T2-hyperintense lesions or simply T2 lesions. White matter T2 lesion load (WM-T2LL) has been reported to be the most relevant predictor of the iron deposition in dGM structures [14]. However, WM-T2LL measurements have generally shown unreliable associations with clinical disability. Most reviewed studies in the literature did not use a multi-parametric, high-resolution, quantitative MRI approach to assess both the dGM structures and WM-T2 lesions in RRMS patients and inter-correlate the extracted MRI measures between them and evaluate their possible associations with disease severity. So we hypothesized that adopting a combined multi-parametric quantitative assessment approach of both the dGM structures and white matter T2 lesions refines a better understanding of the different degrees and aspects of tissue damage in the MS disease process and their association with disease severity.

The objective is to investigate a variety of magnetic resonance imaging (MRI) quantitative metrics, which reflect different aspects of microstructural damage in deep gray matter (dGM) regions and white matter T2 lesions in patients with relapsing-remitting multiple sclerosis (RRMS), and to determine the level of pathological interconnection between these two entities as well as their association with clinical disability.

Materials and methods

Study population

The inclusion criteria for this study were as follows: age between 18 and 65 years; had a clinically definite MS (RRMS) based on revised McDonald's criteria 2010; had not experienced a relapse or received corticosteroid treatment in the last 4 weeks preceding the study; no previous history of other central nervous system's diseases such as demyelinating and neurodegenerative diseases, brain tumor or surgery, head injury, cerebrovascular disease. Thirty patients with RRMS (17 females, 13 males; mean age 31.27 years; age range 20–53 years) who met the inclusion criteria were recruited from the neurology clinic at the Royal Medical Services (RMS) consecutively along with thirty age-matched HCs (16 females, 14 males; mean age 32.35 years; age range 20–54 years). The characteristics of the two study groups are summarized in Table 1. The present study was approved by the RMS ethics committee and carried out in accordance with The Code of Ethics of the World Medical Association (Declaration of Helsinki). All participants gave informed consent according to local ethics approval and fill out the MRI safety questionnaire before participating in the study. Neurological examinations were carried out by a consultant neurologist who was qualified to perform the EDSS assessments according to the standardized scoring system in Neurostatus (http://www.neurostatus.net/scoring/index.php) before the MRI scanning. A functional system (FS) grade was obtained for each area representing a different function of the central nervous system (pyramidal, brain stem, visual, cerebellar, sensory, bowel and bladder, and higher cerebral). The FS scores reflected the degree of disability across all these areas, as found on the neurological assessment. The final EDSS score was calculated on the basis of the combined/summarized FS scores, giving a value of between 0 (normal examination) and 10 (death due to MS) [15].

Magnetic resonance imaging acquisition

MRI scanning was performed on a 3-T Trio system (Siemens Medical Solutions). The imaging protocol included the following imaging sequences: 3D T2-weighted fluid-attenuated inversion recovery (FLAIR) with 1 mm^3 isotropic spatial resolution, reconstruction matrix = 256 × 256, TE = 390 ms, TR = 5000 ms, flip angle = 90°, scan time = 5:52 min; 3D T1-weighted magnetization prepared–rapid acquisition gradient echo (MPRAGE) with 0.9 mm^3 isotropic spatial resolution, reconstruction matrix = 224 × 256, TE = 3.4 ms, TR = 1900 ms, inversion time = 900 ms, flip angle = 9°, scan time = 5:53 min; 3D T2*-weighted gradient echo sequence with 1 mm^3 isotropic spatial resolution, reconstruction matrix = 256 × 256, TE = 20 ms, TR = 33 ms, flip angle = 15°, scan time = 5:30 min; 3D MT-prepared turbo FLASH sequence with spatial resolution = 1 × 1 × 2 mm^3, reconstruction matrix = 256 × 256, TE = 5 ms, TR = 60 ms, flip angle = 10°, scan time = 3.35 min. The same sequence was repeated with similar parameters but with the MT RF pulse "off" (reference volume). T1 maps were created from 3D T1-weighted MPRAGE (short version of MPRAGE or sMPRAGE) images acquired at 8 different inversion times (130, 400, 250, 600, 900, 1200, 1600, 2200 ms) with spatial resolution = 1 × 1 × 3.5 mm^3, reconstruction matrix = 256 × 256, TE = 2.28 ms, TR = 8000 ms, flip angle = 9°, and scan time per inversion time = 2.26 min. Both the MT and T1 images (maps) had a similar anatomical coverage from just above the cingulate gyrus to just below the midbrain (~ 56 mm in the superior-inferior direction).

Table 1 Characteristics of healthy controls (HCs) and relapsing-remitting multiple sclerosis (RRMS) patients

	Subjects	
	RRMS	HCs
Number	30	30
Sex (female/male)	(17/13)	(16/14)
Age range (years)	20–53	20–54
Mean age ± SD (years)	31.27 ± 10.2	32.35 ± 8.7
EDSS range	0–6.5	-
Mean EDSS ± SD	2.67 ± 2.19	-
Number of relapses range	1–8	-
Mean number of relapses	2.9 ± 1.42	-
Time since diagnosis range (months)	1–179	-
Mean of time since diagnosis ± SD (months)	46.03 ± 14.10	-

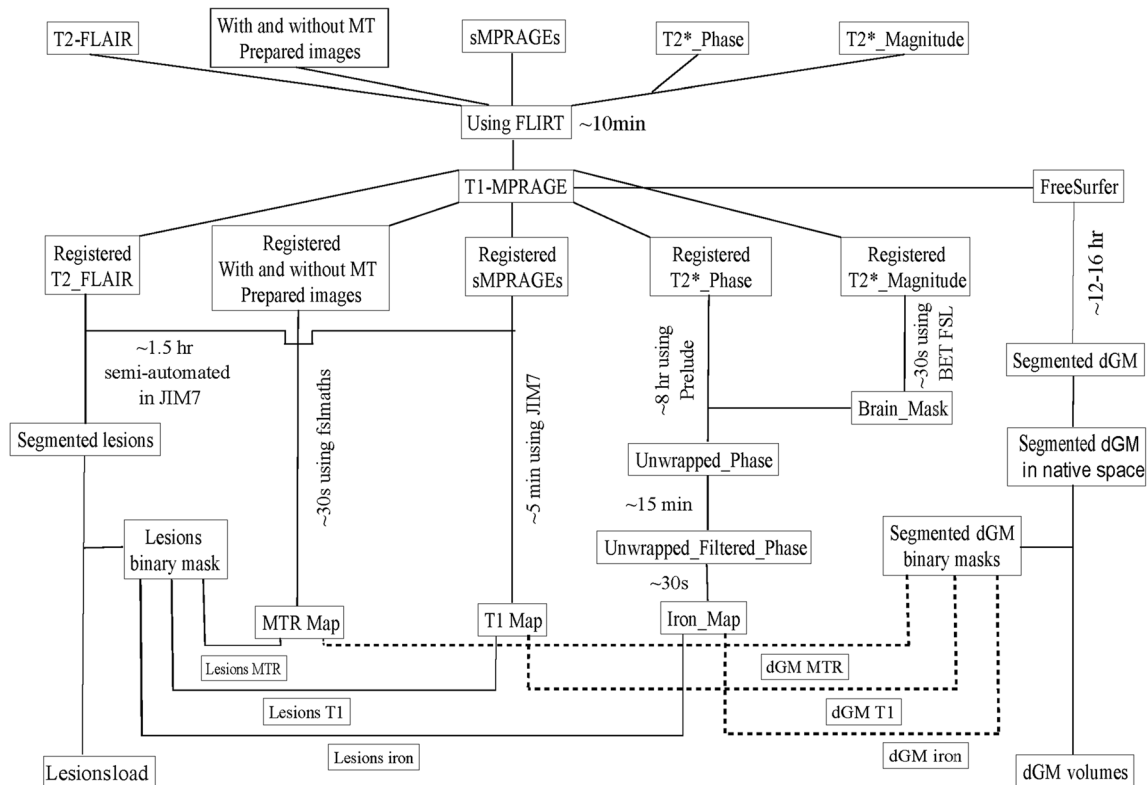SD, standard deviation; EDSS, expanded disability status scale

Fig. 1 Steps of data processing and analysis

Image post-processing and analysis

A summary of image post-processing and analysis steps is shown in Fig. 1.

Calculation of MTR maps

The reference volume from the MT sequence (images acquired with the MT RF pulse "off") was spatially co-registered to the whole head, high-resolution, T1-weighted MPRAGE using the FLIRT linear registration algorithm from the FSL platform (FMRIB). The registration matrix was then applied to the MT volume (images acquired with the MT RF pulse "ON"). The co-registered images were then used to calculate the MTR maps according to the following formula:

$$MTR = \frac{(Reference\ volume - MT\ volume)}{Reference\ volume}$$

Calculation of T1 relaxation time maps

The eight volumes of sMPRAGE images were spatially co-registered to the whole head, high-resolution, T1-weighted MPRAGE with rigid-body image registration using the FLIRT linear registration algorithm from the FSL platform

(FMRIB). The co-registered images were then imported into JIM software (Jim version 7; Xinapse Systems) in which the T1 maps were fitted on a voxel-by-voxel basis.

Calculation of iron concentrations

The magnitude and the phase parts of the T2*-weighted images were spatially co-registered to the high-resolution, T1-weighted MPRAGE using the FLIRT linear registration algorithm from the FSL platform (FMRIB). A whole brain binary mask was produced in FSL, which was then used in Prelude in FMRIB Software Library (FSL) to unwrap the co-registered phase images within the mask. To remove the effects of large-scale background fields, such as those near the air/tissue boundaries at the sinuses, the unwrapped phase data were high-pass-filtered using a dipole fitting method [16]. To calculate iron concentration in dGM structures, the phase differences relative to those of the cerebrospinal fluid (CSF) in the lateral ventricles were converted to iron concentration according to the equation proposed by Haacke (2014): 0.276 radians of the phase difference to be equivalent to 240 μg Fe/g tissue [1]. The phase values of CSF were used as a reference for iron calculation because it is assumed that CSF contains a negligible amount of MR-visible iron. Iron calculations were performed as described in a previous work [15].

Calculation of WM-T2LL

White matter T2 lesion segmentation was performed in JIM software (Jim version 7; Xinapse Systems) as described in the previous work [15]. The segmented MS lesions were masked and used to extract the phase, T1, and MTR values of these MS lesions from the filtered phase, T1, and MTR maps, respectively. The extracted lesions' phase values relative to those of CSF were used to estimate the MS lesions' iron concentration.

Volumetric segmentation of dGM structures in FreeSurfer

The volumetric segmentations of dGM structures were performed with the FreeSurfer image analysis suite [17–19]. The dGM in each hemisphere was segmented into seven subcortical structures (caudate nucleus (CN), putamen (PT), globus pallidus (GP), thalamus (TH), hippocampus, amygdala, and nucleus accumbens) followed by the calculation of their volumes, which were then normalized to the estimated total intracranial volume (eTICV) to account for differences in individual brain sizes. The segmented dGM structures were mapped (converted) from the conformed FreeSurfer space to the native anatomical space "rawavg" space, thresholded (using the structure's label value provided in the FreeSurfer's look-up-table (LUT)), and binarized to extract the corresponding anatomy from the filtered phase, iron, T1, and MTR maps.

Statistical analyses

All statistical analyses were performed in SPSS 23. Data were tested for normality in SPSS using the kurtosis and skewness statistical measures. Data were a little skewed and kurtotic, for both RRMS and HCs, but their skewness and kurtosis z-values were found to be within the normality acceptance range (-1.96 to 1.96) for all quantitative indices in the dGM regions and T2 lesions. As a result, data were assumed to be approximately normally distributed. Differences between patients and controls were assessed using independent samples t test. Correlation coefficients were calculated using Pearson's correlation.

Results

The volumetric measures, magnetization transfer ratios, T1 relaxation times, and iron concentrations of dGM structures of both HCs and RRMS patients are shown in Table 2. A significant statistical difference ($p < 0.01$) was detected between HCs and RRMS patients for the dGM structures with the RRMS showing smaller volumes than HCs. Furthermore, the MTR values of the dGM structures of the RRMS patients

Table 2 Volumetric measures, magnetization transfer ratio (MTR), T1 relaxation time, and iron concentration of deep gray matter structures in RRMS patients and HCs

|	RRMS Mean ± SD	HC Mean ± SD	p value
Volumetric measures			
Normalized CN volume	0.006 ± 0.001	0.008 ± 0.001	< 0.01
Normalized PT volume	0.008 ± 0.001	0.011 ± 0.002	< 0.01
Normalized GP volume	0.002 ± 0.0005	0.003 ± 0.0006	< 0.01
Normalized TH volume	0.011 ± 0.002	0.015 ± 0.002	< 0.01
Mean magnetization transfer ratio			
CN	0.444 ± 0.018	0.635 ± 0.032	< 0.01
PT	0.432 ± 0.041	0.606 ± 0.058	< 0.01
GP	0.423 ± 0.083	0.621 ± 0.090	< 0.01
TH	0.470 ± 0.034	0.665 ± 0.041	< 0.01
Mean T1 relaxation times ± SD (ms)			
CN	1434 ± 144	1359 ± 132	< 0.05
PT	1213 ± 95	1122 ± 122	< 0.01
GP	1034 ± 88	917 ± 107	< 0.01
TH	1177 ± 64	1098 ± 94	< 0.01
Mean iron concentration ± SD (μg)			
CN	36.11 ± 10.86	34.03 ± 18.45	
PT	75.97 ± 20.75	58.30 ± 19.15	< 0.01
GP	23.41 ± 11.22	18.02 ± 7.26	< 0.05
TH	69.31 ± 23.77	82.23 ± 26.94	< 0.05

RRMS, relapsing-remitting multiple sclerosis; *HC*, healthy controls; *SD*, standard deviation; *CN*, caudate nucleus; *PT*, putamen; *GP*, globus pallidus; *TH*, thalamus; *ppm*, parts per million; *ms*, millisecond; *μg*, microgram

were significantly ($p < 0.01$) smaller than those of HCs. Statistically significant differences in T1 relaxation times were detected between the HCs and RRMS patients in the CN ($p < 0.05$), PT, GP, and TH ($p < 0.01$) with the dGM structures of the RRMS patients showing longer T1 times than those of HCs. While RRMS patients showed increased iron deposition in their PT and GP regions, their TH iron levels were significantly ($p < 0.05$) smaller than those of HCs. Plots of differences in normalized volumes, MTR values, T1 relaxation times, and iron concentrations of dGM structures between HCs and RRMS patients are shown in Fig. 2.

Findings illustrated in Table 3 revealed that EDSS had significant positive correlation with the iron concentration in the CN ($r = 0.442$, $p < 0.01$), WM-T2LL ($r = 0.363$, $p < 0.05$), T1 relaxation times of T2 lesions ($r = 0.370$, $p < 0.05$), and iron concentration in the white matter T2 lesions ($r = 0.427$, $p < 0.05$). However, time since diagnosis had significant correlation only with the iron concentration of the CN ($r = 0.452$, $p < 0.05$).

Pearson's correlations of the T2 lesions' quantitative indices with different measures in RRMS patients are shown in Table 4. Significant ($p < 0.05$) moderate associations were

Fig. 2 Plots of differences in (**a**) normalized volumes, (**b**) MTR values, (**c**) T1 relaxation times, and (**d**) iron concentrations of dGM structures between HCs and RRMS patients
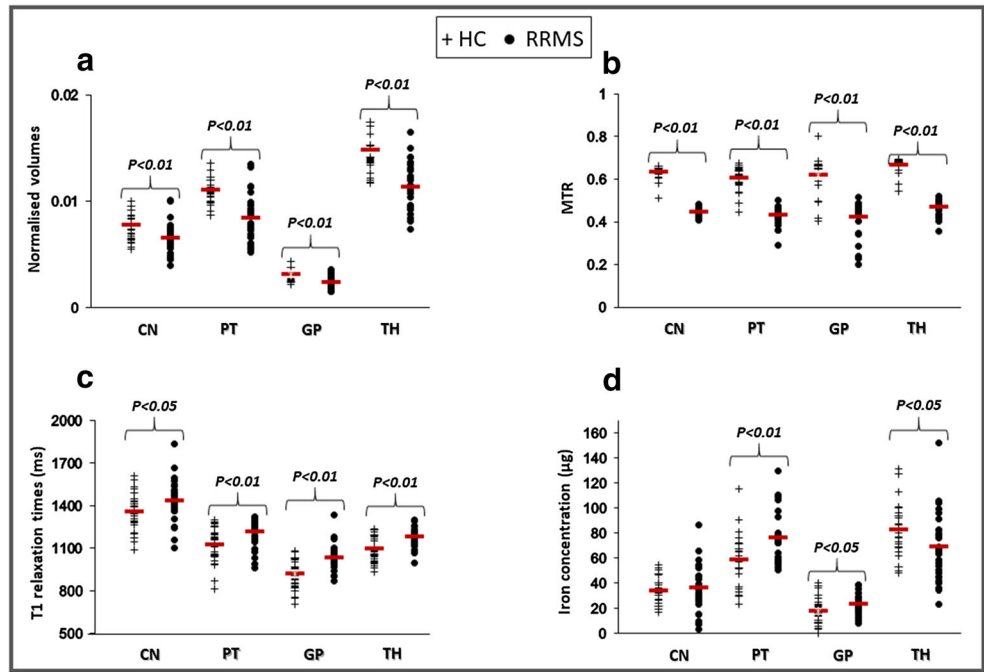
found between the WM-T2LL and atrophy in the PT ($r = -0.408$), GP ($r = -0.410$), and TH ($r = -0.408$). Furthermore, the lesions' MTR values did not associate with any of the calculated quantitative measures. In contrast, dGM

Table 3 Pearson's correlation of the EDSS and time since diagnosis with different deep gray and white matter metrics in RRMS patients

	EDSS		Time since diagnosis (months)	
	r	p value	r	p value
Normalized CN volume	− 0.148	0.22	− 0.002	0.50
Normalized PT volume	− 0.267	0.22	− 0.184	0.17
Normalized GP volume	− 0.134	0.22	− 0.170	0.19
Normalized TH volume	− 0.290	0.06	− 0.270	0.07
MTR of the CN	− 0.244	0.10	− 0.303	0.05
MTR of the PT	− 0.296	0.06	− 0.140	0.23
MTR of the GP	− 0.194	0.15	− 0.078	0.34
MTR of the TH	− 0.221	0.12	− 0.122	0.26
T1 relaxation times of the CN (ms)	0.067	0.36	0.105	0.29
T1 relaxation times of the PT (ms)	0.119	0.27	0.067	0.36
T1 relaxation times of the GP (ms)	0.004	0.49	0.158	0.20
T1 relaxation times of the TH (ms)	0.067	0.36	0.139	0.23
Iron concentration of the CN (μg)	0.442	< 0.01	0.452	< 0.01
Iron concentration of the PT (μg)	0.029	0.44	0.078	0.34
Iron concentration of the GP (μg)	0.006	0.49	− 0.019	0.46
Iron concentration of the TH (μg)	0.183	0.17	− 0.027	0.44
T2 lesion load (mm^3)	0.363	< 0.05	0.192	0.16
MTR of T2 lesions	− 0.078	0.34	− 0.262	0.08
T1 relaxation times of T2 lesions (ms)	0.370	< 0.05	0.256	0.09
Iron concentration of T2 lesions (μg)	0.427	< 0.05	0.295	0.06

EDSS, expanded disability status scale; *MTR*, magnetization transfer ratio; *T1*, longitudinal relaxation time; *T2*, transverse relaxation time; *CN*, caudate nucleus; *PT*, putamen; *GP*, globus pallidus; *TH*, thalamus; *ppm*, parts per million; *ms*, millisecond; *μg*, microgram

Table 4 Pearson's correlations of the T2 lesions' quantitative indices with different measures in RRMS patients

	T2 lesion load (mm³)		MTR of T2 lesions		T1 relaxation times of T2 lesions (ms)		Iron concentration of T2 lesions (µg)	
	r	p	r	p	r	p	r	p
Normalized CN volume	− 0.194	0.15	0.102	0.30	− 0.131	0.25	− 0.292	0.06
Normalized PT volume	− 0.408	< 0.05	0.011	0.48	− 0.082	0.33	− 0.441	< 0.01
Normalized GP volume	− 0.410	< 0.05	0.022	0.45	− 0.032	0.33	− 0.443	< 0.01
Normalized TH volume	− 0.408	< 0.05	0.015	0.47	− 0.049	0.40	− 0.461	< 0.01
MTR of the CN	− 0.061	0.37	0.154	0.24	− 0.480	< 0.01	− 0.193	0.15
MTR of the PT	− 0.064	0.37	0.184	0.38	− 0.510	< 0.01	− 0.171	0.18
MTR of the GP	− 0.030	0.44	0.348	0.38	− 0.449	< 0.01	− 0.074	0.35
MTR of the TH	− 0.038	0.42	0.229	0.41	− 0.478	< 0.01	− 0.141	0.23
T1 relaxation times of the CN (ms)	0.086	0.33	− 0.297	0.26	0.335	< 0.05	0.101	0.30
T1 relaxation times of the PT (ms)	0.063	0.37	− 0.492	0.28	0.333	< 0.05	0.004	0.49
T1 relaxation times of the GP (ms)	0.009	0.48	− 0.404	0.12	0.126	0.25	0.046	0.40
T1 relaxation times of the TH (ms)	0.024	0.45	− 0.484	0.46	0.299	0.06	0.008	0.48
Iron concentration of the CN (µg)	0.262	0.08	− 0.063	0.37	0.115	0.27	0.279	0.07
Iron concentration of the PT (µg)	0.200	0.15	− 0.195	0.15	0.005	0.49	0.159	0.20
Iron concentration of the GP (µg)	0.007	0.49	− 0.020	0.46	0.053	0.39	0.042	0.41
Iron concentration of the TH (µg)	0.258	0.08	− 0.047	0.40	0.008	0.48	0.178	0.17

MTR, magnetization transfer ratio; *T1*, longitudinal relaxation time; *T2*, transverse relaxation time; *CN*, caudate nucleus; *PT*, putamen; *GP*, globus pallidus; *TH*, thalamus; *ms*, millisecond; *µg*, microgram

structures' MTR values showed statistically significant ($p < 0.01$) moderate negative associations with lesions' T1 values. CN and PT's T1 values showed a significant ($p < 0.05$) but weak correlation with lesions' T1 values ($r = 0.335$ and $r = 0.333$, respectively). Significant ($p < 0.01$) moderate associations were found between the lesions' iron concentration and atrophy in the PT ($r = − 0.441$), GP ($r = − 0.443$), and TH ($r = − 0.461$).

Further analysis of the associations between the dGM parametric measures revealed that there is a significant ($p < 0.01$) negative association between the mean T1 relaxation time and MTR in the PT ($r = − 0.706$), GP ($r = − 0.504$), and TH ($r = − 0.0563$) of the RRMS patients.

Discussion

In this study, morphometric, magnetization transfer ratio, T1 relaxation time, and iron concentration changes in dGM structures of both HCs and RRMS patients were investigated using a high-resolution, quantitative, and multi-parametric MRI approach. Similar measurements were derived for the white matter's T2 lesions of the RRMS patients. This multi-parametric approach was adopted with an assumption that different metrics complement each other, and to our knowledge, this is the first study to investigate changes in dGM structures and white matter T2 lesions in a multi-parametric approach using a

composite from a combination of MRI measures (subcortical morphometric measurements, MTR, T1 relaxation times, and iron deposition in both dGM and white matter lesions), derived from high-resolution MR images, to capture different aspects of the MS disease during its relapsing-remitting phase.

Compared with HCs, significant dGM structure atrophy of the RRMS patients was detected in the present study. These findings are in agreement with those reported in other MRI and histopathological studies, which showed that atrophy and demyelinated lesions exist in dGM structures such as the thalamus, hippocampus, caudate, putamen, pallidum, claustrum, hypothalamus, amygdala, and substantia nigra of MS disease [15, 20–24]. None of the measured dGM volumetric metrics showed any association with the EDSS or disease duration although it is not easy to define the disease duration due to the unknown period of asymptomatic disease evolution. Our findings from the previous work showed a significant weak to moderate correlation between the cortical GM atrophy and the EDSS [15]. Other cross-sectional [25, 26] and longitudinal [27, 28] studies have shown a significant association between dGM atrophy and the EDSS. This contradiction could be attributed to their use of larger sample sizes, different segmentation approaches, and anisotropicity of voxel sizes. Except for CN, dGM atrophy was found to be moderately associated with white matter T2 lesions' load and iron concentration. The latter reveals that GM atrophy is associated with white matter injury in multiple sclerosis patients, which could be due to the

association of white matter fibers with different cortical and subcortical GM regions.

The significant reduction in the mean MTR values in all studied dGM structures of the RRMS patients compared with those of age-matched HCs can be attributed to processes such as demyelination, axonal loss, and swelling, which lead to a decrease in the concentration of macromolecules in the MS disease. In RRMS patients, the reduction in dGM MTR values did not significantly associate with the EDSS or disease duration. These findings are in agreement with those found in a study by Amann et al (2015) in which MTR of normal-appearing brain tissues (gray and white matter) did not relate to MS disease severity [29]. However, a study by Davies et al found that cortical gray matter MTR reduction correlates well with disease severity measured using the EDSS [30]. They scanned 38 patients with clinically definite early RRMS at 1.5 T and used a two-dimensional dual-echo interleaved spin echo (SE) MT sequence with a slice thickness of 5 mm. Their patients had minimal or no disability at entry and short disease duration. Data from previous studies regarding MTR changes in DGM are very limited and inconsistent. In addition, MTR measurements lack the standardization across scanners and protocols, which makes the comparison of findings across centers more difficult without further quantification. dGM MTR changes in RRMS were inversely linked only to those of T1 relaxation times in PT, GP, TH, and white matter T2 lesions, but they did not show any association with other quantitative measures within the dGM structures. Although all MTR values of the dGM structures were significantly ($p < 0.01$) inter-correlated, none of them showed any significant correlation with any of the other calculated metrics in the dGM. Furthermore, lesions' MTR values did not associate with the EDSS or disease duration and these findings are different from those found by Amann et al (2015) in which lesions' MTR related to disability in patients with MS better than normal-appearing brain tissue's MTR [29]. Similarly, lesions' MTR values were not linked to those in dGM regions. The latter reveals that white matter and GM fibers undergo demyelination at different rates.

The increased T1 relaxation times in RRMS patients relative to those of HCs are partly in line with other studies in which they found an increase in T1 relaxation time in some, but not all, dGM regions of RRMS as compared with HCs [31, 32]. Niepel et al found that the median T1 relaxation times in the TH and PT only were significantly higher in the RRMS patients than in the HCs. This is partly different from our findings which could be explained by their use of a region of interest analysis approach, which usually does not include the whole anatomical region in the analysis [31]. Although dGM T1 values in PT, GP, and TH were inversely linked to MTR values in these regions, they did not show any association with other quantitative measures in dGM structures, EDSS, or disease duration. It is possible that T1 prolongation

caused by demyelination and gliosis was counteracted by the increased iron deposition detected in most dGM regions. Significant weak correlation was detected between lesions' T1 values and those of CN and PT. Furthermore, lesions' T1 values showed significant moderate negative association with those of dGM MTR.

Findings in this study showed that there was an obvious increase in the iron concentrations in the PT and GP regions of RRMS patients compared with those of HCs. This suggests that iron accumulation occurred in dGM regions during the relapsing-remitting phase of the MS disease. A study by Lommers et al showed that R2* values decreased in dGM regions of RRMS patients compared with those of HCs which indicated decreased iron and myelination levels in these anatomical regions [33]. They attributed the decrease in iron concentrations in dGM regions of RRMS patients to the fact that their RRMS patients were younger than HCs. However, R2* measurement might be affected by other effects such as changes in water or myelin density. Thalamic iron seems to follow different rules than iron in other dGM structures and its relation to the clinical outcomes of MS is still indistinct. A significant reduction in iron concentration was found in the TH of RRMS patients as compared with that of HCs. The latter could be attributed to the involvement of chronic microglia activation in the depletion of iron from oligodendrocytes in this central and integrative brain region [34]. Reduced thalamic iron detected in this study is in line with findings by Zivadinov et al (2018) in which reduced thalamic iron was observed in MS patients compared with HCs and attributed to a reduced iron content of damaged oligodendrocytes that would release iron under stress conditions [35]. No significant connections were detected between any of the dGM iron concentrations and other quantitative metrics in dGM structures, white matter lesions, EDSS, or disease duration. Other studies showed a good correlation between iron levels in dGM regions and the EDSS [26, 35–37]. Our findings were partially contradictory to their findings which could be attributed to their use of larger sample sizes, different iron estimation methods, and anisotropicity of voxel sizes. Contrarily to dGM regions, lesions' iron concentration showed a significant moderate correlation with the EDSS and dGM atrophy.

In this study, we dedicated special attention to obtaining accurate dGM segmentations that are consistent throughout our multimodal dataset. In addition, quantitative maps were created carefully using relatively robust methods which were tested and optimized for accurate measurements of specific imaging parameters. Furthermore, the high-resolution, multiparametric approach used in this study bridges many gaps in the understanding of the hidden dGM tissues' changes. Moreover, extracting the same quantitative indices from both dGM structures and white matter T2 lesions provides important information about the pathological changes within these regions and how they are interrelated.

Although a larger sample size is required to validate these findings and understand their potential clinical impact, we believe that the findings of the current study could add some knowledge on the pathological changes of the MS disease during the relapsing-remitting phase and the strategic approaches of magnetic resonance imaging that should be adopted in the future studies. GM atrophy was found to associate with white matter injury in our patients; this linkage shows that there might be a significant association of white matter fibers with different cortical and subcortical GM regions. The latter can be further exploited using fiber tractography. Furthermore, WM and GM fibers were found to undergo demyelination at different rates, which could be due to different microstructural components or pathological processes of MS disease. In addition, dGM and lesions' quantitative measures tend to occur in a non-homogenous pattern and to different degrees and their associations with MS disease severity are so different. These findings urge adopting a new approach of imaging in large cohort of MS patients in which a whole brain, high-resolution, quantitative scans are preformed and different parametric maps are created so that a global as well as regional quantitative measure can be extracted and assessed collectively. These maps can also be evaluated before and after drug therapy so that the effect of these drugs can be better assessed by detecting different MRI quantitative measures in the brain, either globally or in specific regions.

The main limitation of the current study was the relatively small sample size. So, additional studies with a larger number of RRMS patients and more MS phenotypes, such as primary and secondary progressive MS, are required to validate these findings. In addition, this study used a single imaging time point, and as a result it lacks information about how parametric changes evolve over time. Furthermore, the clinical assessment protocol at the neurologic clinic did not include a detailed cognitive test for MS patients which prevented us from testing any possible associations between some MRI indices and MS patients' cognitive ability. The large variation in the disease duration at the time of participation might have affected the results and it can be considered as an additional limitation, and careful selection of MS patients with a more homogeneous range of disease duration is important in future research.

In conclusion, dGM structures are very much involved in the MS disease process and quite substantial neurodegeneration is undergone during the relapsing-remitting phase of the MS disease. In addition, dGM quantitative changes occur in a non-uniform and non-linked pattern and, except for CN's iron deposition, do not directly associate with the MS disease severity. In contrast, most white matter lesions' metrics tend to correlate with MS disease severity better than those of dGM structures.

Compliance with ethical standards

Guarantor The scientific guarantor of this publication is Dr. Ali Al-Radaideh (The Hashemite University, Jordan).

Conflict of interest The authors of this manuscript declare no relationships with any companies whose products or services may be related to the subject matter of the article.

Statistics and biometry No complex statistical methods were necessary for this paper.

Informed consent Written informed consent was obtained from all subjects (patients) in this study.

Ethical approval Institutional Review Board approval was obtained.

Study subjects or cohorts overlap Some study subjects or cohorts have been previously reported in Al-Radaideh et al 2019, Reference No. [15] in the manuscript.

Methodology
• prospective
• case-control study
• performed at one institution

References

1. Haacke EM, Reichenbach J (2011) Susceptibility weighted imaging in MRI: basic concepts and clinical applications, 1st edn. Wiley-Blackwell, Hoboken
2. Schoonheim MM, Popescu V, Lopes FCR et al (2012) Subcortical atrophy and cognition: sex effects in multiple sclerosis. Neurology 79:1754–1761
3. Calabrese M, Rinaldi F, Grossi P et al (2010) Basal ganglia and frontal/parietal cortical atrophy is associated with fatigue in relapsing-remitting multiple sclerosis. Mult Scler 16:1220–1228
4. Wolff SD, Balaban RS (1994) Magnetization transfer imaging: practical aspects and clinical applications. Radiology 192:593–599
5. Cercignani M, Bozzali M, Iannucci G, Comi G, Filippi M (2001) Magnetisation transfer ratio and mean diffusivity of normal appearing white and grey matter from patients with multiple sclerosis. J Neurol Neurosurg Psychiatry 70:311–317
6. Fernando KTM, Tozer DJ, Miszkiel KA et al (2005) Magnetization transfer histograms in clinically isolated syndromes suggestive of multiple sclerosis. Brain 128:2911–2925
7. Khaleeli Z, Sastre-Garriga J, Ciccarelli O, Miller DH, Thompson AJ (2007) Magnetisation transfer ratio in the normal appearing white matter predicts progression of disability over 1 year in early primary progressive multiple sclerosis. J Neurol Neurosurg Psychiatry 78:1076–1082
8. Dehmeshki J, Chard DT, Leary SM et al (2003) The normal appearing grey matter in primary progressive multiple sclerosis. J Neurol 250:67–74

9. Rovaris M, Bozzali M, Santuccio G et al (2001) In vivo assessment of the brain and cervical cord pathology of patients with primary progressive multiple sclerosis. Brain 124:2540–2549

10. Peterson JW, Bö L, Mörk S, Chang A, Trapp BD (2001) Transected neurites, apoptotic neurons, and reduced inflammation in cortical multiple sclerosis lesions. Ann Neurol 50:389–400

11. Dutta R, Chang A, Doud MK et al (2011) Demyelination causes synaptic alterations in hippocampi from multiple sclerosis patients. Ann Neurol 69:445–454

12. Wegner C, Esiri MM, Chance SA, Palace J, Matthews PM (2006) Neocortical neuronal, synaptic, and glial loss in multiple sclerosis. Neurology 67:960–967

13. Al-Radaideh AM, Wharton SJ, Lim S-Y et al (2013) Increased iron accumulation occurs in the earliest stages of demyelinating disease: an ultra-high field susceptibility mapping study in Clinically Isolated Syndrome. Mult Scler 19:896–903

14. Raz E, Branson B, Jensen JH et al (2015) Relationship between iron accumulation and white matter injury in multiple sclerosis: a case–control study. J Neurol 262:402–409

15. Al-Radaideh A, Athamneh I, Alabadi H, Hbahbih M (2019) Cortical and subcortical morphometric and iron changes in relapsing-remitting multiple sclerosis and their association with white matter T2 lesion load. Clin Neuroradiol 29:51–64

16. Wharton S, Schäfer A, Bowtell R (2010) Susceptibility mapping in the human brain using threshold-based k-space division. Magn Reson Med 63:1292–1304

17. Fischl B, Salat DH, Busa E et al (2002) Whole brain segmentation: automated labeling of neuroanatomical structures in the human brain. Neuron 33:341–355

18. Dale AM, Fischl B, Sereno MI (1999) Cortical surface-based analysis: I. Segmentation and surface reconstruction. Neuroimage 9: 179–194

19. Fischl B, Sereno MI, Dale AM (1999) Cortical surface-based analysis. II: inflation, flattening, and a surface-based coordinate system. Neuroimage 9:195–207

20. Ramasamy DP, Benedict RHB, Cox JL et al (2009) Extent of cerebellum, subcortical and cortical atrophy in patients with MS. J Neurol Sci 282:47–54

21. Vercellino M, Plano F, Votta B, Mutani R, Giordana MT, Cavalla P (2005) Grey matter pathology in multiple sclerosis. J Neuropathol Exp Neurol 64:1101–1107

22. Vercellino M, Masera S, Lorenzatti M et al (2009) Demyelination, inflammation, and neurodegeneration in multiple sclerosis deep gray matter. J Neuropathol Exp Neurol 68:489–502

23. Gilmore CP, Donaldson I, Bo L, Owens T, Lowe J, Evangelou N (2009) Regional variations in the extent and pattern of grey matter demyelination in multiple sclerosis: a comparison between the cerebral cortex, cerebellar cortex, deep grey matter nuclei and the spinal cord. J Neurol Neurosurg Psychiatry 80:182–187

24. Datta S, Staewen TD, Cofield SS et al (2015) Regional gray matter atrophy in relapsing remitting multiple sclerosis: baseline analysis of multi-center data. Mult Scler Relat Disord 4:124–136

25. Shiee N, Bazin PL, Zackowski KM et al (2012) Revisiting brain atrophy and its relationship to disability in multiple sclerosis. PLoS One. https://doi.org/10.1371/journal.pone.0037049

26. Hagemeier J, Weinstock-Guttman B, Heininen-Brown M et al (2013) Gray matter SWI-filtered phase and atrophy are linked to disability in MS. Front Biosci (Elite Ed) 5:525–532

27. Eshaghi A, Marinescu RV, Young AL et al (2018) Progression of regional grey matter atrophy in multiple sclerosis. Brain 141:1665–1677

28. Eshaghi A, Prados F, Brownlee WJ et al (2018) Deep gray matter volume loss drives disability worsening in multiple sclerosis. Ann Neurol 83:210–222

29. Amann M, Papadopoulou A, Andelova M et al (2015) Magnetization transfer ratio in lesions rather than normal-appearing brain relates to disability in patients with multiple sclerosis. J Neurol 262:1909–1917

30. Davies GR, Ramió-Torrentà L, Hadjiprocopis A et al (2004) Evidence for grey matter MTR abnormality in minimally disabled patients with early relapsing-remitting multiple sclerosis. J Neurol Neurosurg Psychiatry 75:998–1002

31. Niepel G, Tench CR, Morgan PS, Evangelou N, Auer DP, Constantinescu CS (2006) Deep gray matter and fatigue in MS. J Neurol 253:896–902

32. Steenwijk MD, Vrenken H, Jonkman LE et al (2016) High-resolution T1-relaxation time mapping displays subtle, clinically relevant, gray matter damage in long-standing multiple sclerosis. Mult Scler 22:1279–1288

33. Lommers E, Simon J, Reuter G et al (2019) Multiparameter MRI quantification of microstructural tissue alterations in multiple sclerosis. NeuroImage Clin. https://doi.org/10.1016/j.nicl.2019.101879

34. Schweser F, Martins ALRD, Hagemeier J et al (2018) Mapping of thalamic magnetic susceptibility in multiple sclerosis indicates decreasing iron with disease duration: a proposed mechanistic relationship between inflammation and oligodendrocyte vitality. Neuroimage 167:438–452

35. Zivadinov R, Tavazzi E, Bergsland N et al (2018) Brain iron at quantitative MRI is associated with disability in multiple sclerosis. Radiology 289:487–496

36. Neema M, Arora A, Healy BC et al (2009) Deep gray matter involvement on brain MRI scans is associated with clinical progression in multiple sclerosis. J Neuroimaging 19:3–8

37. Ropele S, Kilsdonk ID, Wattjes MP et al (2014) Determinants of iron accumulation in deep grey matter of multiple sclerosis patients. Mult Scler 20:1692–1698